Acta Neuropathol (2002) 103:428–436
DOI 10.1007/s00401-001-0485-5

REGULAR PAPER

Róbert Adalbert · József I. Engelhardt · László Siklós

DL-Homocysteic acid application disrupts calcium homeostasis and induces degeneration of spinal motor neurons in vivo

Received: 9 May 2001 / Revised: 27 July 2001 / Accepted: 3 October 2001 / Published online: 23 February 2002

Abstract Excitotoxicity, autoimmunity and free radicals have been postulated to play a role in the pathomechanism of amyotrophic lateral sclerosis (ALS), the most frequent motor neuron disease. Altered calcium homeostasis has already been demonstrated in Cu/Zn superoxide dismutase transgenic animals, suggesting a role for free radicals in the pathogenesis of ALS, and in passive transfer experiments, modeling autoimmunity. These findings also suggested that yet-confined pathogenic insults, associated with ALS, could trigger the disruption of calcium homeostasis of motor neurons. To test the possibility that excitotoxic processes may also be able to increase calcium in motor neurons, we applied the glutamate analogue DL-homocysteic acid to the spinal cord of rats in vivo and analyzed the calcium distribution of the motor neurons over a 24-h survival period by electron microscopy. Initially, an elevated cytoplasmic calcium level, with no morphological sign of degeneration, was noticed. Later, increasing calcium accumulation was seen in different cellular compartments with characteristic features of alteration at different survival times. This calcium accumulation in organelles was paralleled by their progressive degeneration, which culminated in cell death by the end of the observation time. These findings confirm that increased calcium also plays a role in excitotoxic lesion of motor neurons, in line with previous studies documenting the involvement of calcium ions in motor neuronal injury in other models of the disease as well as elevated calcium in biopsy samples from ALS patients. We suggest that intracellular calcium might be responsible for the interplay between the different pathogenic processes resulting in a uniform clinicopathological picture of the disease.

R. Adalbert · L. Siklós (✉)
Institute of Biophysics, Biological Research Center,
P.O. Box 521, 6701 Szeged, Hungary
e-mail: siklos@nucleus.szbk.u-szeged.hu,
Tel.: +36-62-432080170, Fax: +36-62-433133

J.I. Engelhardt
Department of Neurology, University of Szeged,
Szeged, Hungary

Keywords Calcium · Excitotoxicity · Motor neuron · DL-Homocysteic acid

Introduction

Amyotrophic lateral sclerosis (ALS) is a neurodegenerative disorder characterized by progressive loss of upper and lower motor neurons, leading to paralysis, respiratory failure and death [14]. ALS occurs in both sporadic (sALS) and familial (fALS) forms, which are clinically and pathologically similar. Many theories have been proposed to account for the selective degeneration of motor neurons in ALS (for review see [17, 33]), including the involvement of autoimmune mechanisms [1], oxidative stress [28], excitotoxicity [30], and cytoskeletal abnormalities [12]. Although the cause of the disease is unknown and there is only limited understanding of the mechanisms of motor neuron loss, research data have suggested the importance of impaired calcium homeostasis in motor neuron injury. In our previous studies we found increased calcium accumulation in motor nerve terminals of sALS patients [36]. Experimentally, similar changes were induced in mice injected with immunoglobulins (IgG) isolated from sALS patients [8]. Modification of the calcium distribution within spinal motor neurons was also documented in a transgenic mouse model of familial ALS, based on the $G^{93}\rightarrow A$ mutation of the gene encoding Cu/Zn superoxide dismutase (SOD-1) [38]. Although several studies have demonstrated the importance of excitotoxic mechanism in ALS [24, 29, 30, 31], so far no data are available to show the calcium distribution at subcellular level in excitatory amino acid-induced motor neuron degeneration. In the present experiments, ultrastructural techniques were used to analyze whether changes in the calcium homeostasis are associated with excitotoxic motor neuron injury. To evoke degeneration of spinal motor neurons, rats were injected subdurally with DL-homocysteic acid (DL-HCA), an excitatory amino acid analogue of glutamate, which has been shown to induce severe lesions in motor neurons over a time scale of several hours [15].

The alterations in the distribution of intracellular calcium in the spinal motor neurons, paralleling these pathological changes, were then monitored at various survival intervals electron microscopically using the oxalate-pyroantimonate-glutaraldehyde fixation method [3, 4].

Materials and methods

In vivo excitatory amino acid application

Male, 21-day-old CFY rats were used for the experiments. Animals were anesthetized with intraperitoneal injection of a mixture of xylazine (12 mg/kg) and ketamine (108 mg/kg). An incision was made over the lower thoracic and lumbar spine, the paraspinal muscles were dissected and, to expose the lumbar spinal cord, the posterior arches of the upper lumbar vertebrae were removed over two to three segments. Following the posterior laminectomy, 730 μg DL-HCA was subdurally injected (10 μl 400 mM DL-HCA in distilled water, pH adjusted to 7.4 with NaOH). Immediately after the injection the skin was sutured and the animals were allowed to recover. Control rats were operated and injected with 10 μl distilled water (pH adjusted to 7.4) in the same way. All the experiments were performed in accordance with institutional guidelines for animal experiments and with governmental laws for animal protection (protocol no. 72/k-6/1999).

Specimen preparation and electron microscopy

Animals were allowed to survive for 1, 3, 6, or 24 h following DL-HCA injection, and then, under anesthesia, they were transcardially perfused with 3% glutaraldehyde containing 90 mM oxalic acid adjusted to pH 7.4 with KOH [3, 4]. Ten animals were used at each survival time. Spinal cords were dissected, cut into segments and fixed for additional 12 h in the same fixative. Following post-fixation in 1% osmic acid containing 2% potassium pyroantimonate, spinal cord samples were dehydrated in graded series of ethanol, processed through propylene oxide and embedded in Durcupan ACM. Blocks were polymerized for 2 days at 56°C, then semithin sections with 0.5-μm nominal thickness were cut on a Sorvall MT 5000 ultramicrotome, stained according to Richardson [27] and examined under the light microscope (Olympus Vanox T) to localize large motor neurons. After trimming the blocks to the ventrolateral motor neuron pool, ultrathin (40–50 nm thick) sections were cut, mounted on formvar-coated single-hole copper grids, stained with uranyl acetate [11] and lead citrate [26] and examined in a Zeiss CEM 902 electron filtering microscope. The applied fixation procedure ensured good structural preservation and resulted in electron-dense deposits (EDDs) due to the reaction with tissue calcium. These reaction products were easily discernible under the transmission electron microscope. To guarantee the specificity of the histochemical procedure, the composition of EDDs was regularly controlled by electron spectroscopic imaging (ESI) [2] using the digital image analysis system (IBAS 2.0, Kontron) attached to the microscope. For such analysis, 20- to 30-nm unstained sections were prepared, significant calcium distribution was determined in randomly selected regions of the sections, then the calcium distribution pattern was correlated with the distribution of the EDDs. To perform the ESI analysis, individual images were recorded at ×20,000–30,000 by 80 kV accelerating voltage of the microscope, using a 90-μm objective aperture and a 650-μm spectrometer entrance aperture with a slit width of 8–10 eV. Element-specific (at the ionization edge of calcium) and background image pairs were recorded at energy loss values of 355 eV and 310 eV, respectively. Between 500 and 600 video images were recorded and averaged for each energy loss value to produce low noise images for further calculations. Next, the net calcium distribution was determined by subtracting the background image from

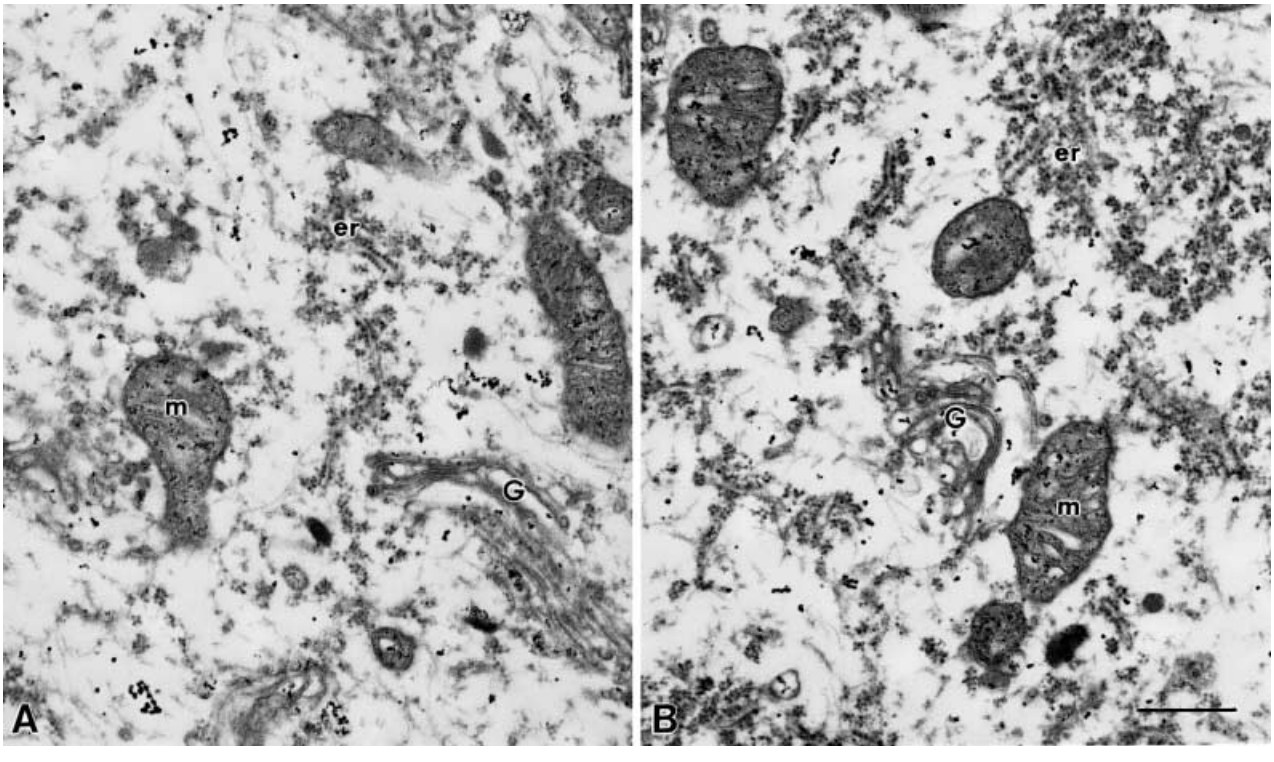

Fig. 1 **A** Electron micrograph of a motor neuron from the lumbar section of spinal cords of 21-day-old untreated control rats displays no structural alteration and low level of calcium. **B** At 0-h survival time the ultrastructural appearance is similar to the control, i.e., neither morphological changes nor elevated calcium are seen (*m* mitochondrion, *ER* endoplasmic reticulum, *G* Golgi apparatus). Oxalate-pyroantimonate reaction; *bar* 0.5 μm

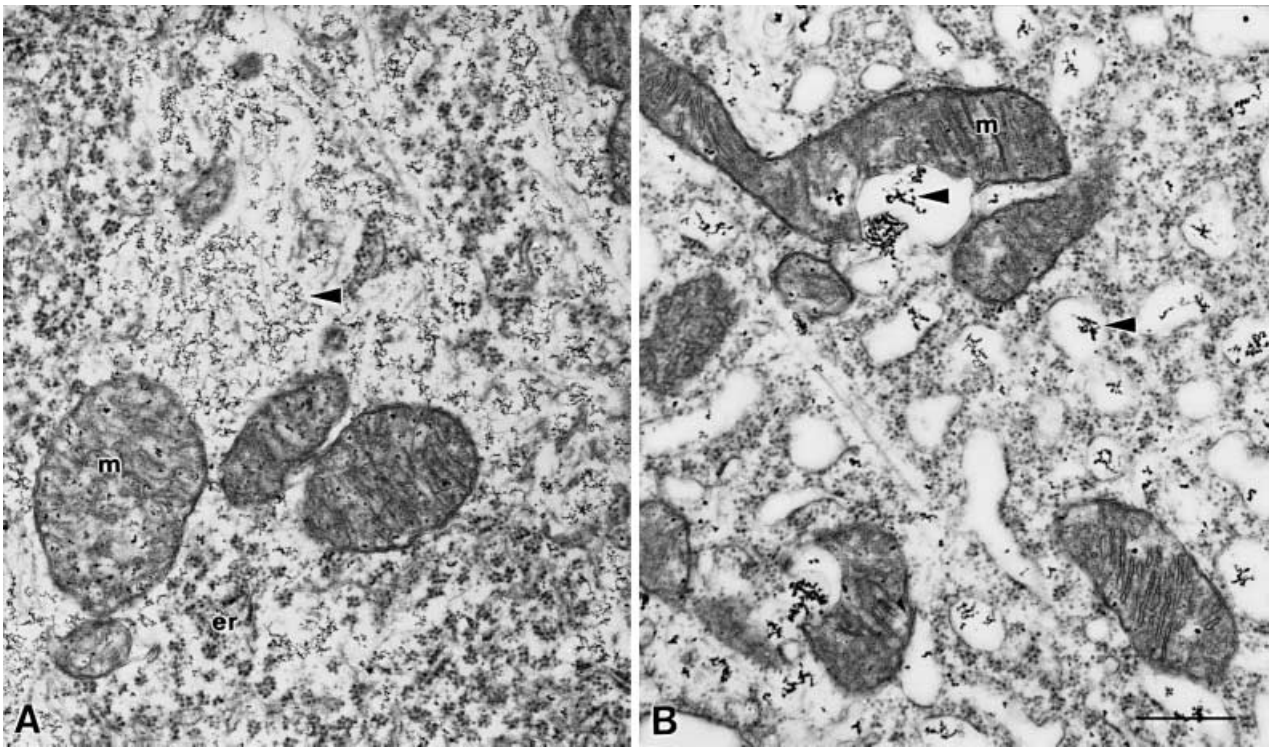

Fig. 2A, B Electron micrographs of motor neurons from the lumbar section of the spinal cord of DL-HCA injected rats at 1-h survival time after the injection. **A** Generally, no structural alteration is seen, but regularly an elevated level of cytoplasmic calcium is present. **B** Occasionally initial signs of degeneration can be observed affecting mainly the ER, which has dilated cisterns and calcium precipitates. The majority of mitochondria are uninfluenced, with localized calcium accumulation only (DL-HCA DL-homocysteic acid, *m* mitochondrion, *arrowhead* calcium deposits). Oxalate-pyroantimonate reaction; *bar* 0.5 μm

the "edge" image. The significant calcium distribution pattern was visualized by color-coding the difference image according to the mean +2.5 SD – mean +6 SD rule. Using this method, pixels identifying a significant signal (i.e., significantly above the average) were colored and retained in the analytical image, while non-significant signals were eliminated. To check the correlation of the true calcium distribution with the pattern of the EDDs, this color-coded image was finally superimposed onto the black-and-white fine-structural digital image of the same area, recorded at the carbon absorption edge (dE=250 eV).

Results

Ultrastructural alterations and the accompanying changes of the calcium distribution of spinal motor neurons were analyzed at different time points up to 24 h following DL-HCA injection. When the animals were killed immediately after the DL-HCA application (0-h survival time), neither degenerative alterations, nor changes in the calcium distribution (Fig. 1B) compared to the untreated controls (Fig. 1A) were seen. Similarly, no ultrastructural changes were observed following subdural injection of distilled water, used as the vehicle of DL-HCA in our experiments.

By 1 h following DL-HCA injection the majority of motor neurons either showed no changes, or only cytoplasmic calcium accumulation was present (Fig. 2A). However, in a few cases initial signs of degeneration were noticed, with dilatation of cisterns of the endoplasmic reticulum (ER) and Golgi complex, paralleled with calcium accumulation. In such neurons the majority of mitochondria showed normal ultrastructure with spatially restricted calcium uptake only (Fig. 2B).

Generally, a large variance of the reactions of motor neurons were noticed at each time point following DL-HCA application. This heterogeneity was most apparent after 3 h survival, when it ranged from a slight elevation of calcium paralleled with mild or no injury, to a robust calcium increase and definite degeneration. At this time point, according to their overall appearance, we arbitrarily sorted the motor neurons into three groups with signs of either (1) modest, (2) advanced or (3) profound degeneration. In the first group (modest injury) morphological changes were rarely noticed. At most, an increased calcium accumulation in the cytoplasm was documented (Fig. 3A), compared to controls (Fig. 1A), while intracellular organelles did not show elevated levels of calcium. In the second group (advanced lesion) morphological changes were significant in the majority of motor neurons. Although all the cytoplasmic organelles were affected in some way, large variations were observed with regards to the distinct features of the degeneration and the actual distribution of intracellular calcium. In some of the neurons the degeneration involved mainly the ER and the Golgi apparatus in such a way that they exhibited an increased calcium content (Fig. 3B), while the neighboring mitochondria displayed calcium content comparable to controls (cf. Fig. 1A, Fig. 3B). In some other motor neu-

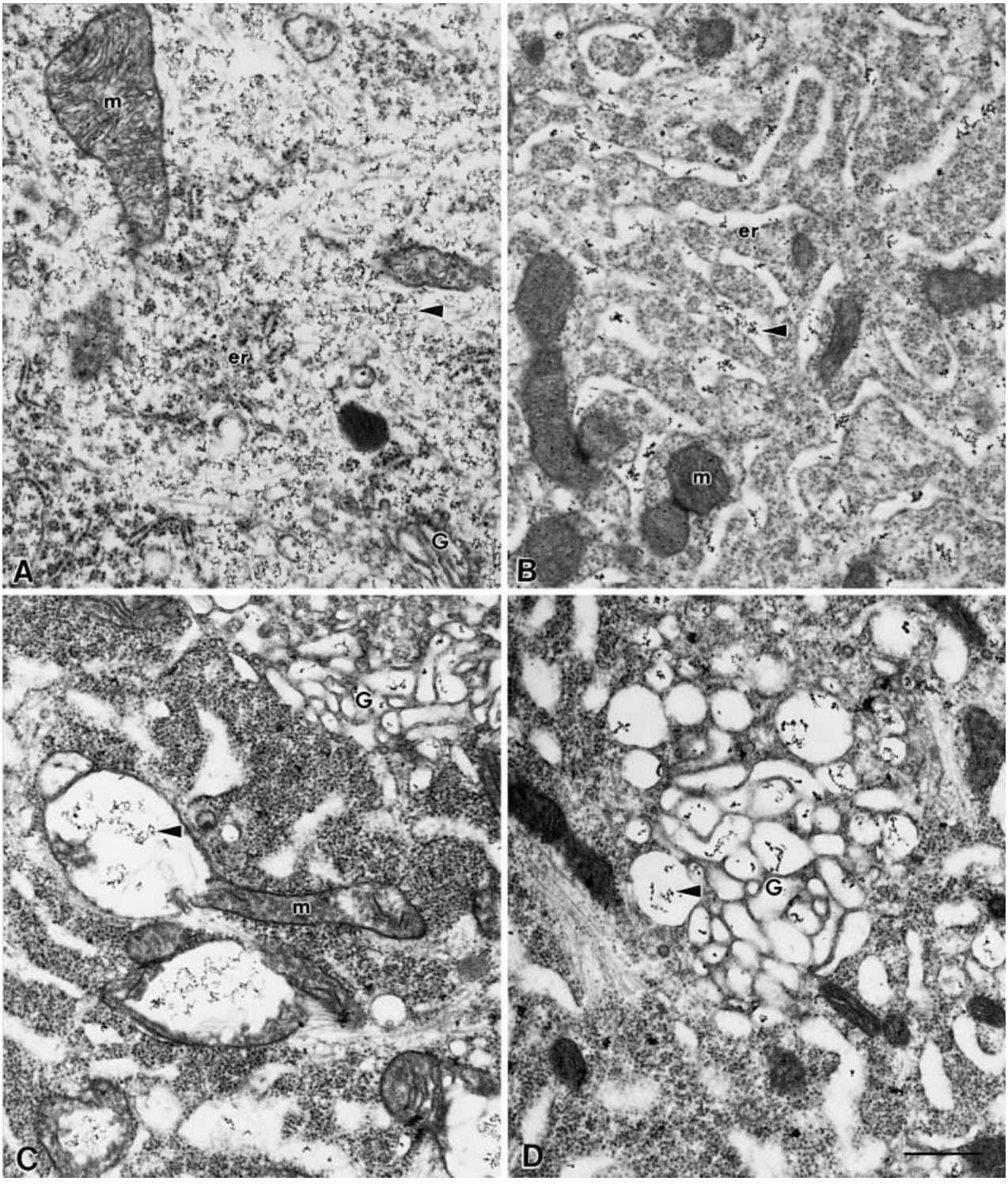

Fig. 3A–D Electron micrographs of spinal motor neurons from a DL-HCA-injected rat in different stages of degeneration 3 h following injection. **A** Early phase of degeneration (modest stage). While the structural integrity of motor neurons is not changed, a cytoplasmic calcium increase can be detected. **B** Advanced degeneration. Cisterns of the ER are dilated and contain calcium deposits. Mitochondria are somewhat compressed, likely due to the osmotic pressure originating from the dilatation of the neighboring organelles; however, their membrane structure is intact; furthermore, they contain EDDs comparable to the control only (Fig. 1A). **C** Advanced degeneration. Localized mitochondrial swelling and calcium accumulation is seen, while the neighboring swollen ER and Golgi complex contain no, or minimal amount of calcium. **D** Profound degeneration. At this stage of degeneration an advanced vacuolization is seen. The vacuoles may originate from the ER or from the fragmented Golgi system. In most of the cases these vacuoles contain clusters of precipitates, while the shrunken and dark mitochondria are regularly devoid of calcium (*EDDs* electron-dense deposits, *m* mitochondrion, *ER* endoplasmic reticulum, *G* Golgi apparatus, *arrowhead* calcium deposits). Oxalate-pyroantimonate reaction; *bar* 0.5 μm

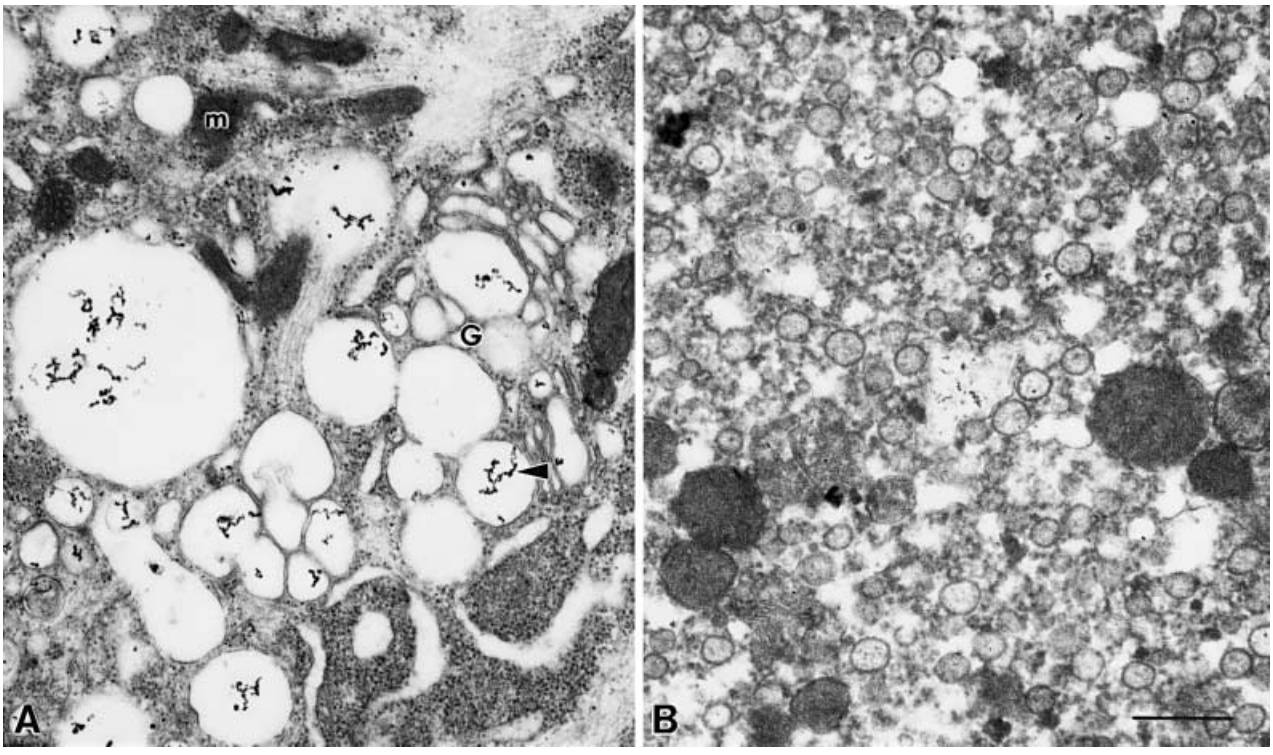

Fig. 4A, B Electron micrographs of motor neurons from the lumbar section of the spinal cord of DL-HCA-injected rats at 6- and 24-h survival times after the injection. **A** At 6 h survival time profound structural alterations are seen with advanced vacuolization of the Golgi complex and the ER, paralleled by calcium accumulation, while the mitochondria are regularly shrunken and dark with no visible calcium. **B** At 24 h following DL-HCA injection a total disintegration of the cytoplasmic structure is seen, and most of the organelles are degenerated beyond recognition (*m* mitochondrion, *G* Golgi apparatus, *arrowhead* calcium deposits). Oxalate-pyroantimonate reaction; *bar* 0.5 μm

rons, a contrasting picture could be seen: mitochondrial calcium accumulation and partial swelling (Fig. 3C) was paralleled by the depletion of calcium from the adjacent organelles. Finally, a rather homogeneous calcium uptake was also observed, with elevated calcium level in both swollen mitochondria and dilated cisterns of the nearby structures. In the third group (profound degeneration), the cytoplasm of motor neurons regularly contained vacuoles of different sizes (Fig. 3D), which were identified as dilated fragments of the Golgi apparatus or cistern of the ER system. In most of the cases, but not always, these vacuoles contained clusters of calcium precipitates. Unlike these organelles, all the perikaryonal mitochondria appeared dark and shrunken, with significantly decreased or absent calcium content.

At 6 h after the injection, strong fragmentation and vacuolization of both the endoplasmic reticulum system and the Golgi apparatus was documented (Fig. 4A). Various-sized clusters of calcium precipitates were regularly present in the enlarged, swollen cisternae of the organelles. At this survival time mitochondria were typically dark and shrunken, with no visible EDDs inside. Generally, the ultrastructure and the calcium distribution of these neurons was similar to those in the third group (profound degeneration) of the 3-h material (Fig. 3D).

By 24 h following DL-HCA injection most of the motor neurons had lost their structural integrity and only few of the cytoplasmic organelles remained recognizable (Fig. 4B). Nearly all of the organelles had lost their normal conformation, and were fragmented and degenerated beyond recognition. Very low calcium level was only seen within the neurons at this stage of degeneration.

An interesting aspect of the present results is the recognition that, at least in this excitotoxicity model, mitochondria are able to exert a non-homogeneous volumetric response to the environmental stress when either the mitochondrial swelling or the mitochondrial calcium uptake is considered. We detected mitochondria with local swelling and increased calcium in this small swollen volume fraction, affecting only a very small proportion of the actual mitochondrial volume (Fig. 5A, B). In addition, mitochondria in which swelling and calcium uptake extended to a dominant proportion of the mitochondrial volume were observed. However, in these mitochondria the remaining volume fraction showed normal ultrastructure and low level of calcium (Fig. 5C, D). Finally, mitochondria were also observed with increased calcium distributed homogeneously in the swollen mitochondrial volume (Fig. 5E, F).

Discussion

In the present experiments DL-HCA, an excitotoxic analogue of glutamate that interacts with both NMDA and non-NMDA receptor subtypes, was used to trigger the de-

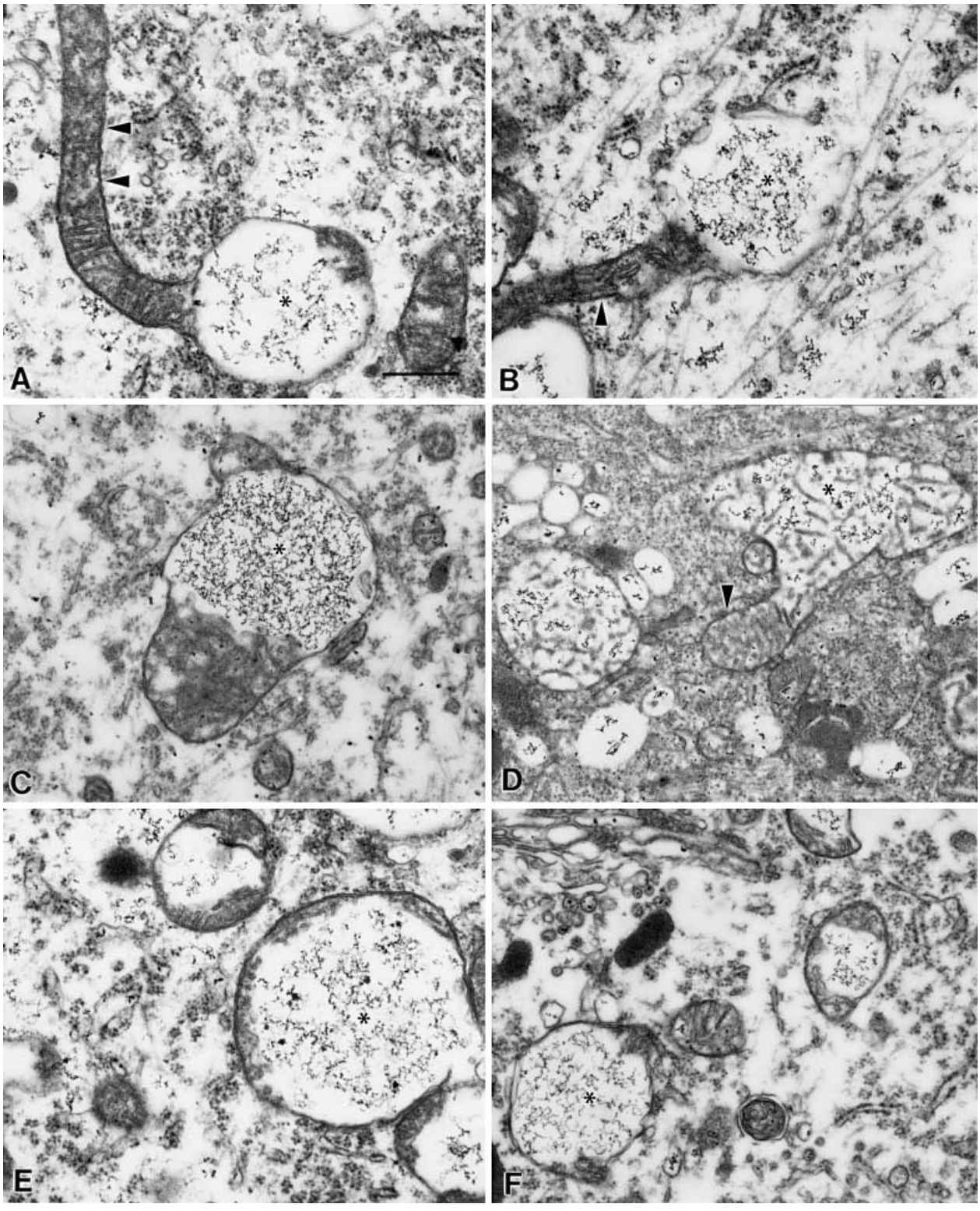

Fig. 5A–F Electron micrographs of mitochondria in different stages of degeneration with various amounts of calcium. **A**, **B** According to the proposed sequence of alterations, during the first phase the structural disintegration and the calcium accumulation are local (*asterisks*); the majority of the mitochondrial volume has a normal structure (*arrowheads*). **C**, **D** Next, a more advanced swelling, paralleled by an increased calcium accumulation can develop (*asterisks*), which results in a marked decrease of intact mitochondrial volume (*arrowhead* in **C**). **E**, **F** Finally, mitochondria reach a state with extensive swelling and ample calcium uptake (*asterisks*). It is suggested that mitochondrial swelling does not take places uniformly throughout the mitochondria, but propagates along a direction within the mitochondria; furthermore, since the electron microscopy technique could capture these differently evolved conditions, it is likely that they can exist for a prolonged time. Oxalate-pyroantimonate reaction; *bar* 0.5 μm

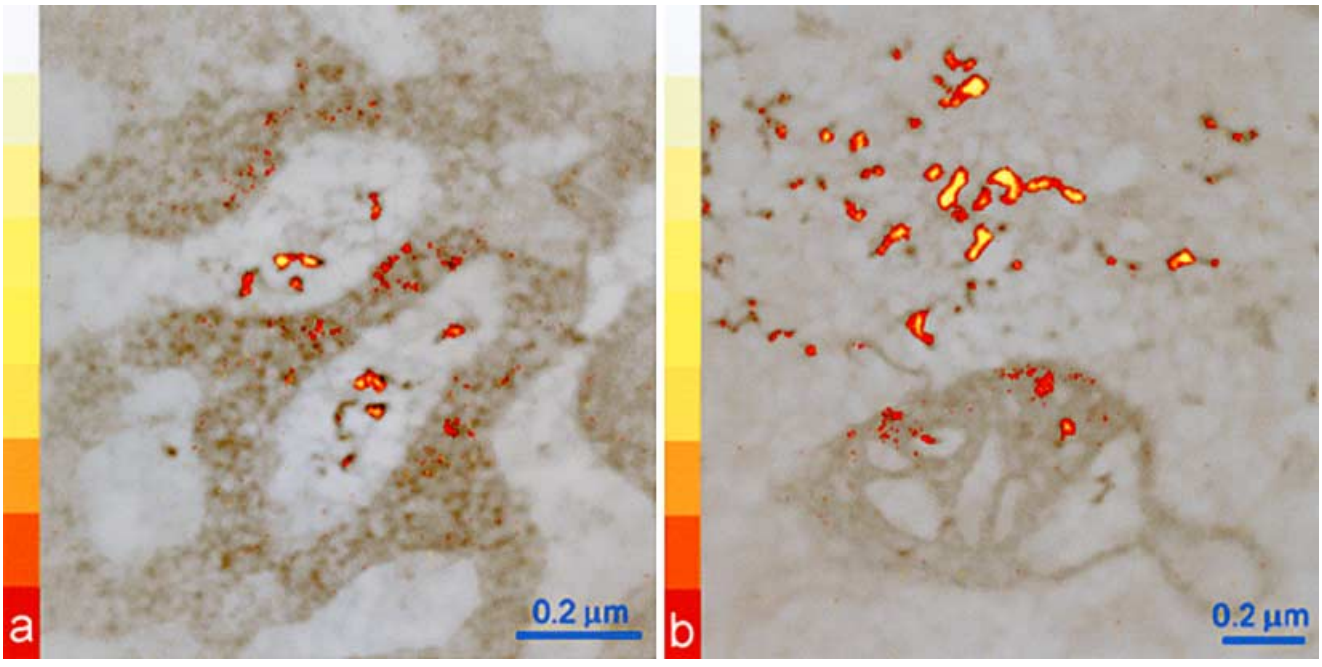

Fig. 6a, b Analytical proof of the calcium content of the electron-dense precipitates obtained with the oxalate-pyroantimonate procedure. Calcium distribution was determined by the electron spectroscopic imaging method and exemplified in two randomly selected fields. **a** Dilated cisterns of the ER with internal calcium precipitates; **b** partially swollen mitochondrion surrounded by scattered cytoplasmic calcium deposits. The significant calcium signal was color coded according to the actual significance value at each pixel above the 2.5 SD significance level (*red*) up to the 6.0 SD value (*white*). The true (*colored*) calcium signal can be adequately correlated with the EDDs

generation of motor neurons. DL-HCA was effective in inducing a robust injury of spinal motor neurons and, unlike kainate or AMPA [15], was well tolerated by the animals during the 24-h survival period. Spasms of the tail and hindlimbs were seen for 1–2 min immediately after the subdural injection of DL-HCA, likely due to a strong hyperactivation of lumbar motor neurons, but no further clinical sign of the effect of the excitotoxin was noted during the whole observed period. Several attempts have been made to optimize the dose and the method of application of DL-HCA. First, direct drainage of DL-HCA to the exposed spinal cord was tested, after removing the dura [15], and then different concentrations/dosages of the compound were examined. However, reproducible results were obtained only using subdural injection, and only at a dose not smaller than 700 µg DL-HCA. Furthermore, no immediate reactions of the animals were noticed, suggesting hyperexcitation, when lower doses of the drug were injected. In control rats, injected with distilled water alone, neither clinical signs of motor dysfunction, nor pathological/ultrastructural alteration of motor neurons were observed. Since the ultrastructural pathology of the spinal cord after a similar acute and invasive application of DL-HCA has already been extensively described [15], we confined our study to following the alterations of motor neurons and to determining the concurrent changes in their intracellular calcium distribution.

The credibility of our results, describing the modification of the intracellular calcium distribution during degeneration of motor neurons following an excitotoxic insult, depends fundamentally on the histochemical fixation. The oxalate-pyroantimonate preparation procedure, to fix and visualize the subcellular distribution of calcium, provides good ultrastructural preservation and does not induce structural alterations, as we described earlier [37]. Furthermore, the specificity of the histochemical reaction for calcium has already been confirmed with energy dispersive X-ray microanalysis [5], and electron spectroscopic imaging [6, 8, 9, 35, 36]. Finally, the procedure proved to be applicable to following function-dependent changes of neuronal calcium distribution not only in our hands [38], but also in other laboratories [21, 25]. Nevertheless, the calcium content of the EDDs was regularly checked and verified during the present study using the ESI method [2] (Fig. 6a, b).

We noticed a great diversity in the reaction of motor neurons after subdural injection of DL-HCA when the ultrastructural alterations or the calcium distribution were observed. Besides the biological variations, this heterogeneity might be largely attributed to methodological problems, such as unintended, slight, but nonreproducible physical injury of the spinal cord during the removal of the posterior arches of the vertebrae, or uneven diffusion of the DL-HCA into the tissue. However, the time course analysis helped to reconstruct the conceivable sequence of the alteration of the ultrastructure and calcium distribution from the initial step of the degeneration until the cell death. In the earliest stage, neither calcium accumulation, nor ultrastructural changes were seen (Fig. 1B). Later, when structural alterations still could not be noticed, elevated calcium levels were detected in the cytoplasm of

motor neurons, while the organelles were unaffected, having calcium content comparable to the controls (Figs. 2A, 3A). Next, a redistribution of the intracellular calcium from the cytoplasm to membrane-enclosed organelles started, mainly to the ER and mitochondria (Figs. 2B; 3B, C), which was accompanied by a gradual conformational change of these structures (dilatation of the cisternae, fragmentation). Before the final disintegration and elimination of the calcium content of the cells (Fig. 4B), a progressive degeneration of the organelles was seen (Figs. 2, 3). At this stage, the gravity point of the calcium distribution could be set either to mitochondria, or to the ER/Golgi apparatus, or to both. Nevertheless, accepting that at the time of fixation individual neurons might be at differently advanced stages in the course of degeneration, this scenario could be brought in accord with the cooperative role of the ER and mitochondria in handling of intracellular calcium [13].

As the appropriate surface receptors are activated, calcium influx and release from the internal stores (due to the activation of the inositol triphosphate receptors of the ER) could lead to an increase of the intracellular calcium [34]. Consecutively, mitochondrial calcium uptake takes place, even under physiological conditions [39], preferably at those microdomains where the ER and mitochondria are at intimate proximity (see Fig. 2B) [22]. If the calcium load is high enough, however, a biphasic mitochondrial calcium uptake can be induced, at least in vitro [13], before the final collapse of the mitochondrial homeostasis occurs. In the first phase, this uptake is not paralleled by detectable mitochondrial swelling [13], which might correspond to those mitochondria in our material where only local calcium accumulation could be seen (Figs. 2B; 5A, B). The second phase, accompanied by gradual swelling of the organelles (Figs. 3C; 5C–F) could eventually lead to opening of mitochondrial permeability transition pore in its high conductance state, release of matrix calcium and disintegration of the organelles (Figs. 3D, 4A). Although an ATP-dependent reload of the ER stores could take place parallel to these mitochondrial events (Fig. 3B), the collapse of mitochondrial ATP synthesis should also induce a secondary depletion of such stores. Finally, the mitochondrial permeability transition leads to the release of apoptosis-inducing factors, which results in apoptotic or necrotic cell death, depending on the available energy (ATP) of the actual cell [18, 23] (Fig. 4B). Our results indicate that a cytoplasmic calcium increase followed by a relocation of calcium to mitochondria are essential steps leading to excitotoxic motor neuronal death. These findings are also supported by in vitro experiments, in which a similar sequence of changes in the intracellular calcium were documented, irrespective of whether apoptotic or necrotic type of cell death was induced [19].

Our present study has been aimed at analyzing the role of calcium in a model of ALS, a prototype of motor neuron diseases. During previous investigations of human biopsy material using electron microscopic histochemistry we documented an elevated level of mitochondrial and vesicular calcium in motor nerve terminals from biceps muscles of sALS patients [36]. These findings were corroborated in subsequent experiments employing the passive transfer model of sALS, by demonstrating a calcium increase not only in motor axon terminals of the interosseus muscle, but also in the cell bodies of spinal motor neurons [8]. The most authentic models for fALS are based on transgenic animals carrying the same mutations of the SOD-1 gene taht were detected in a subpopulation of the ALS patients [10]. Applying the calcium histochemistry technique to this model, we also documented a gradual elevation of intracellular calcium in spinal, but not in parvalbumin-rich oculomotor neurons, which was paralleled by their different degeneration [38]. As an extension of these studies, in the present experiments we showed an increased level of calcium in spinal motor neurons after application of a glutamate analogue, suggesting an important role of the impairment of the calcium homeostasis during excitotoxicity (another well-accepted model of sALS [16]). Assuming that ALS may be a multifactorial disease [7], on the basis of the above results, we suggest that alteration in the intracellular calcium level and/or distribution might be the crucial element in its pathomechanism. Appropriate changes in the subcellular calcium concentration could result in the proliferation and synchronization of a variety of distress conditions and, irrespective of the actual initiating element, could lead to a uniform clinical picture of the disease. Indeed, data are already available indicating a calcium-dependent interplay of the excitotoxic injury and the degeneration of motor neurons induced by the mutant SOD-1 enzyme [32]. Furthermore, an increased glutamate level in the cerebrospinal fluid of rats was demonstrated in the passive transfer model of sALS [20], suggesting an interaction of immune-mediated and excitotoxic processes. Further studies aimed at experimentally influencing the stability of motor neuronal calcium homeostasis, e.g., through the regulation of certain calcium binding proteins, like parvalbumin or calbindin D-28K, may help to prove the pivotal role of calcium ions in the pathomechanism of ALS.

Acknowledgements This work was supported by the National Scientific Research Fund of Hungary (OTKA T 026239, T 034314, M 36252), the Hungarian Ministry of Welfare (ETT T04/001/2000, T05/028/2000), the Hungarian Ministry of Higher Education (FKFP 0032/2000) and the US-Hungary Science and Technology Fund (JF-661).

References

1. Appel SH, Alexianu ME, Engelhardt JI, Siklós L, Smith RG, Mosier D, Mohamed H (2000) Involvement of immune factors in motor neuron cell injury in amyotrophic lateral sclerosis. In: Brown RH Jr, Meininger V, Swash M (eds) Amyotrophic lateral sclerosis. Martin Dunitz, London, pp 309–326
2. Bauer R (1988) Electron spectroscopic imaging: an advanced technique for imaging and analysis in transmission electron microscopy. Methods Microbiol 20:113–146
3. Borgers M, De Brabander DM, Van Reempts DJ, Awouters F, Jacob WA (1977) Intranuclear microtubules in lung mast cells of guinea pigs in anaphilactic shock. Lab Invest 37:1–8

4. Borgers M, Thoné EF, Van Neuten JM (1981) The subcellular distribution of calcium and effects of calcium antagonists as evaluated with a combined oxalate-pyroantimonate technique. Acta Histochem S24:327–332
5. Dux E, Kloiber O, Hossmann KA, Siklós L (1987) Calcium in hippocampus following lidocaine-induced seizures: an electron cytochemical study. Acta Biol Hung 38:213–224
6. Dux E, Oschiles U, Uto A, Kusumoto M, Siklós L, Joó F, Hossmann KA (1996) Serum prevents glutamate-induced mitochondrial calcium accumulation in primary neuronal cultures. Acta Neuropathol 92:264–272
7. Eisen A (1995) Amyotrophic lateral sclerosis is a multifactorial disease. Muscle Nerve 18:741–752
8. Engelhardt JI, Siklós L, Kömüves L, Smith RG, Appel SH (1995) Passive transfer of amyotrophic lateral sclerosis (ALS) immunoglobulin to mice selectively increases intracellular calcium and induces ultrastructural changes in motor neurons. Synapse 20:185–199
9. Engelhardt JI, Siklós L, Appel SH (1997) Altered calcium homeostasis and ultrastructure in motor neurons of mice caused by passively transferred anti-motoneuronal IgG. J Neuropathol Exp Neurol 56:21–39
10. Gurney ME (2000) Transgenic animal models of amyotrophic lateral sclerosis. In: Brown RH Jr, Meininger V, Swash M (eds) Amyotrophic lateral sclerosis. Martin Dunitz, London, pp 251–262
11. Hayat MA (1970) Principles and techniques of electron microscopy, vol 1. Biological applications. Van Nostrand Reinhold, New York, pp 264–274
12. Hirano A (1991) Cytopathology of amyotrophic lateral sclerosis. Adv Neurol 56:91–101
13. Ichas F, Mazat JP (1998) From calcium signaling to cell death: two conformations for the mitochondrial permeability transition pore. Switching from low to high conductance state. Biochim Biophys Acta 1366:33–50
14. Ince P (2000) Neuropathology. In: Brown RH Jr, Meininger V, Swash M (eds) Amyotrophic lateral sclerosis. Martin Dunitz, London, pp 83–112
15. Ikonomidou C, Qin QY, Labruyere J, Olney JW (1996) Motor neuron degeneration induced by excitotoxins agonists has features in common with those seen in the SOD-1 transgenic mouse model of amyotrophic lateral sclerosis. J Neuropathol Exp Neurol 55:211–224
16. Jackson M, Rothstein JD (2000) Excitotoxicity in amyotrophic lateral sclerosis. In: Brown RH Jr, Meininger V, Swash M (eds) Amyotrophic lateral sclerosis. Martin Dunitz, London, pp 263–278
17. Julien JP (2001) Amyotrophic lateral sclerosis: unfolding the toxicity of the misfolded. Cell 104:581–591
18. Kroemer G, Dallapporta B, Resche-Rigon M (1998) The mitochondrial death/life regulator in apoptosis and necrosis. Annu Rev Physiol 60:619–642
19. Kruman II, Mattson MP (1999) Pivotal role of mitochondrial calcium uptake in neural cell apoptosis and necrosis. J Neurochem 72:529–540
20. LaBella V, Goodman JC, Appel SH (1997) Increased CSF glutamate following injection of ALS immunoglobulins. Neurology 48:1270–1272
21. Mata M, Staple J, Fink DJ (1986) Changes in intra-axonal calcium distribution following nerve crush. J Neurobiol 17: 449–467
22. Mattson MP, LaFerla FM, Chan SL, Leissring MA, Shepel PN, Geiger JD (2000) Calcium signaling in the ER: its role in neuronal plasticity and neurodegenerative disorders Trends Neurosci 23:222–229
23. Nicotera P, Lipton SA (1999) Excitotoxins in neuronal apoptosis and necrosis. J Cereb Blood Flow Metab 19:583–591
24. Plaitakis A (1991) Altered glutamatergic mechanisms and selective motor neuron degeneration in amyotrophic lateral sclerosis: possible role of glycine. Adv Neurol 56:319–326
25. Pullen AH, Humphreys P (2000) Ultrastructural analysis of spinal motor neurons from mice treated with IgG from ALS patients, healthy individuals, or disease controls. J Neurol Sci 180:35–45
26. Reynolds ES (1963) The use of lead citrate at high pH as an electron-opaque stain in electron microscopy. J Cell Biol 17: 208–212
27. Richardson KC, Jarett L, Finke EH (1960) Embedding in epoxy resins for ultrathin sectioning in electron microscopy. Stain Technol 35:313–323
28. Rosen DR, Siddique T, Patterson D, et al (1993) Mutation in Cu/Zn superoxide dismutase are associated with familial amyotrophic lateral sclerosis. Nature 362:59–62
29. Rothstein JD, Martin LJ, Kuncl RW(1992) Decreased glutamate transport by the brain and spinal cord in amyotrophic lateral sclerosis. N Engl J Med 326:1464–1468
30. Rothstein JD, Van Kammen M, Levey AI, Martin LJ, Kuncl RW (1995) Selective loss of glial glutamate transporter GLT-1 in amyotrophic lateral sclerosis. Ann Neurol 38:73–84
31. Rothstein JD, Dykes-Hoberg M, Pardo CA, Bristol LA, Jin L, Kuncl RW, Kanai Y, Hediger MA, Wang Y, Schielke JP, Welty DF (1996) Knock-out of glutamate transporters reveals a major role for astroglial transport in excitotoxicity and clearance of glutamate. Neuron 16:675–686
32. Roy J, Minotti S, Dong L, Figlewicz DA, Durham HD (1998) Glutamate potentiates the toxicity of mutant Cu/Zn-superoxide dismutase in motor neurons by postsynaptic calcium-dependent mechanisms. J Neurosci 18:9673–9684
33. Shaw PJ, Eggett CJ (2000) Molecular factors underlying selective vulnerability of motor neurons to neurodegeneration in amyotrophic lateral sclerosis. J Neurol 247 [suppl 1]:17–27
34. Siesjö BK, Hu B, Kristián T (1999) Is the cell death pathway triggered by the mitochondrion or the endoplasmic reticulum? J Cereb Blood Flow Metab 19:19–26
35. Siklós L, Kuhnt U (1994) Calcium accumulation by dendritic mitochondria declines along the apical dendrites of pyramidal neurons in area CA1 of guinea pig hippocampal slices. Neurosci Lett 173:131–134
36. Siklós L, Engelhardt J, Harati Y, Smith RG, Joó F, Appel SH (1996) Ultrastructural evidence for altered calcium in motor nerve terminals in amyotrophic lateral sclerosis. Ann Neurol 39:203–216
37. Siklós L, Kuhnt U, Párducz Á, Szerdahelyi P (1997) Intracellular calcium redistribution accompanies changes in total tissue Na^+, K^+, and water during the first two hours of in vitro incubation of hippocampal slices. Neuroscience 79:1013–1022
38. Siklós L, Engelhardt JI, Alexianu ME, Gurney ME, Siddique T, Appel SH (1998) Intracellular calcium parallels motor neuron degeneration in SOD-1 mutant mice. J Neuropathol Exp Neurol 57:571–587
39. Werth JL, Thayer SA (1994) Mitochondria buffer physiological calcium loads in cultured rat dorsal root ganglion neurons. J Neurosci 14:348–356